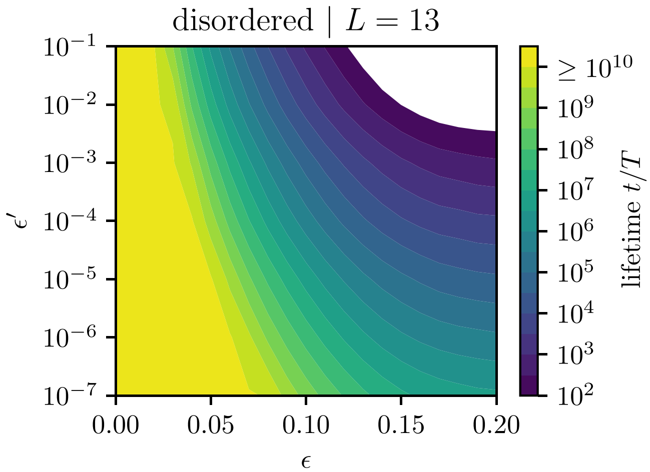

FIG. 8. The disorder-averaged lifetimes of the global chain z magnetization with $N = 13$ spins, starting in the fully polarized initial state. The data were obtained by numerical sigmoid fits. Lifetimes above $\geqslant 10^{10}T$ and below $\leqslant 10^2T$ cannot be adequately resolved.

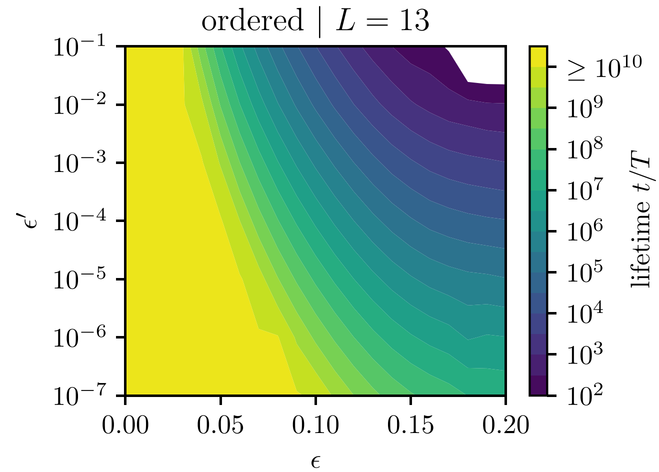

FIG. 9. The lifetimes of the global ordered-chain z magnetization with $N = 13$ spins, starting in the fully polarized initial state. The data were obtained through numerical cosine fits. Lifetimes above $\geqslant 10^{10}T$ and below $\leqslant 10^2T$ cannot be adequately resolved.

Heisenberg XX and XXZ models, could lead to new insights into out-of-equilibrium dynamics in quantum many-body systems.

ACKNOWLEDGMENTS

We thank Matthias Weidemüller, Roderich Mössner, Sebastian Geier, and Razvan Gurau for fruitful discussions. This work is supported by the Deutsche Forschungsgemeinschaft (DFG, German Research Foundation) under Germany's Excellence Strategy EXC2181/1-390900948 (the Heidelberg STRUCTURES Excellence Cluster) and within the Collaborative Research Center SFB1225 (ISOQUANT). The authors acknowledge support by the state of Baden-Württemberg through bwHPC and the DFG through Grant No. INST 40/575-1 FUGG (Helix and JUSTUS2 clusters). For the numerical work, we used the JULIA programming language [55].

APPENDIX A: DISORDERED COUPLINGS AND FIELDS

The stabilization mechanism proposed in Sec. III A is not based on the presence of disorder in the system. To study the interplay of disorder with the metronome, we repeat the drive-parameter scan of Fig. 3 for a disordered system. Specifically, we subject a polarized initial state to realizations of the Hamiltonian of Eq. (1), where the parameters $J_{i,i+1}$ and h_i are uniform iid random variables according to $J_{i,i+1} \sim \mathcal{U}(0.5, 1.5)$ and $h_{i,} \sim \mathcal{U}(-1, 1)$, in analogy to simulations shown in Ref. [5]. The resulting average over 250 disorder realizations of the Floquet unitary is shown in Fig. 8. Since the increase in complexity due to the disorder average required a reduction in the size of the system to $L = 13$, we also give the analogous data set for a disorder-free chain of the same length in Fig. 9. The averaged time traces approximately follow a sigmoid shape $\propto 1/(1 + \exp \alpha t)$, as different disorder realizations have different Rabi oscillation frequencies and cancel out at late times. The times plotted in Fig. 8 correspond to $t = 1/\alpha$, so the magnetization has decreased to $\sim 1/(1 + e) \approx 26.9\%$ of the plateau value. Comparing the two figures reveals that the behavior is qualitatively the same. However, making direct quantitative comparisons between the two data sets is not directly possible due to the differences discussed in the determination of the lifetime.

APPENDIX B: METRONOME SPIN AT THE CENTER OF THE CHAIN

Up until now, we have studied systems with the metronome attached to the end of a linear chain or to the side of it, coupled to the central spin of the chain. Now, we replace a central spin on the index $i = \lfloor (L + 1)/2 \rfloor =: m$, i.e., $\epsilon_m = \epsilon'$. For odd chain lengths (here $L = 13$), the spin is exactly in the middle of the chain, and the system has a spatial inversion symmetry, reducing the numerical complexity. The global z magnetization of a polarized initial state is depicted in Fig. 10. The global magnetization of the centrally stabilized system has many similarities with that of the original setup with stabilization at the boundary, as shown in Fig. 2. The system demonstrates Rabi oscillations with a similar frequency and initial magnetization amplitude. However, after $\approx 10^5$ Floquet drive cycles, the metronome-spin magnetization temporarily decays to the chain average (right axis) in Fig. 10, before the subsequent Rabi oscillations set in.

The metronome is coupled to two neighboring spins subjected to the standard drive angle deviation, ϵ, instead of the previous single spin. Therefore, the observed reduced time of the initial decay compared to the boundary metronome is consistent with this difference in chain configuration. Before that decay, the dynamics of the metronome can, in good approximation, again be considered to be largely independent of the rest of the chain. Thus, the metronome effectively decouples the two half-chains, acting as a rotating field on its two neighbors. After the decay, the two chains are coupled